



Electrical energy wireless transfert: Application to electric roads

Mehdi Rouissiya, Ikram El Abbassi, Bilal Amghar, Alain Jaafari, A.-Moumen Darcherif, Abdallah Saad

► To cite this version:

Mehdi Rouissiya, Ikram El Abbassi, Bilal Amghar, Alain Jaafari, A.-Moumen Darcherif, et al.. Electrical energy wireless transfert: Application to electric roads. 15th International Conference on Electrical Machines, Drives and Power Systems (ELMA 2017), Jun 2017, Sofia, Bulgaria. pp.309-313, 10.1109/ELMA.2017.7955454 . hal-02016085

HAL Id: hal-02016085

<https://hal.science/hal-02016085>

Submitted on 12 Feb 2019

HAL is a multi-disciplinary open access archive for the deposit and dissemination of scientific research documents, whether they are published or not. The documents may come from teaching and research institutions in France or abroad, or from public or private research centers.

L'archive ouverte pluridisciplinaire **HAL**, est destinée au dépôt et à la diffusion de documents scientifiques de niveau recherche, publiés ou non, émanant des établissements d'enseignement et de recherche français ou étrangers, des laboratoires publics ou privés.

Electrical Energy Wireless Transfert: Application to Electric Roads.

Mehdi ROUSSIYA, Ikram El Abbassi, Bilal Amghar
 ECAM-EPMI
 Quartz Laboratory
 Cergy-Pontoise, France
 m.rouissiya@ecam-epmi.fr
 i.elabbassi@ecam-epmi.fr
 b.amghar@ecam-epmi.fr

Pr. Alain JAAFARI, Pr. A.-Moumen DARCHERIF,
 *Pr. Abdallah SAAD
 ECAM-EPMI
 Quartz Laboratory
 Cergy-Pontoise, France
 a.jaafari@ecam-epmi.fr
 m.darcherif@ecam-epmi.fr
 *ENSEM- Casablanca
 saad.abdal@gmail.com

Abstract—The present paper focuses on wireless energy transfer mechanisms applied to urban electric vehicles. It describes the using conditions of a particular transformer without ferromagnetic core, supplied by a resonant inverter and loaded by mobile sources (catenaries with magnetic induction to power electric vehicles). The system consists of unconventional transformers with large air-gaps and a generator who supplies the transformer. The paper describes the theoretical model used for the numerical simulation (magnetic circuit, power converter, loads), and the measurements provided by our experimental platform (Tesla lab.). The transformer is supplied by a half-bridge series resonant converter. The transformer secondary coil is mobile compared to the primary, which is fixed on the road. This system is found in many industrial applications such as light automatic vehicles, tramways, etc. In this work we will show that the performance of a transformer without magnetic circuit can be equivalent to a standard transformer.

Keywords—Power Electronic; Wireless Power Transfer; Electric vehicles; Electric road; Coupling circuits; Mutual coupling; Resonant inverters

I. INTRODUCTION

Many manufacturers of electric vehicles have shown interest in wireless power transfer technology, also known as inductive power transfer, for the development of the electric vehicle market. Several studies and prototypes have been carried out, making contactless power transfer technology mature enough, so that manufacturers can make functional solutions with it, especially for the electric vehicles charging. Nevertheless, research into wireless power transfer is deepened in order to overtake the static charging and be able to make a dynamic batteries charging. This will allow increasing the autonomy of the electric vehicles by a partial and fast charge during their movement.

Our aim consists of transmitting maximum power through air-gaps transformer for a given geometric configuration and a given vertical separation distance Z_0 (see figure 1). The transformer is made up of two coils in Litz wire. The primary is fixed. The movements of the secondary are assumed to be parallel to the primary in a 3D space.

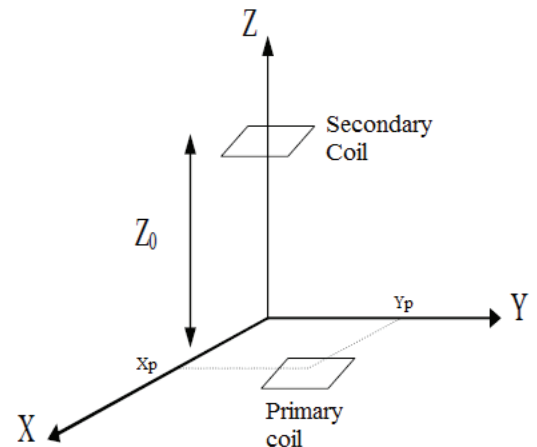


Fig.1. Spatial configuration of the transformer

Contactless energy transfer system operates at resonance. Indeed a half bridge series resonant converter supplies the primary of the transformer as shown on figure 2. This allows a soft commutation of the switches which is an important precondition for reaching higher transmission frequencies. The soft commutation of Mosfets is realized by the intermediary of an assistance system to commutation. Therefore switching events are achieved at zero voltage (ZVS).

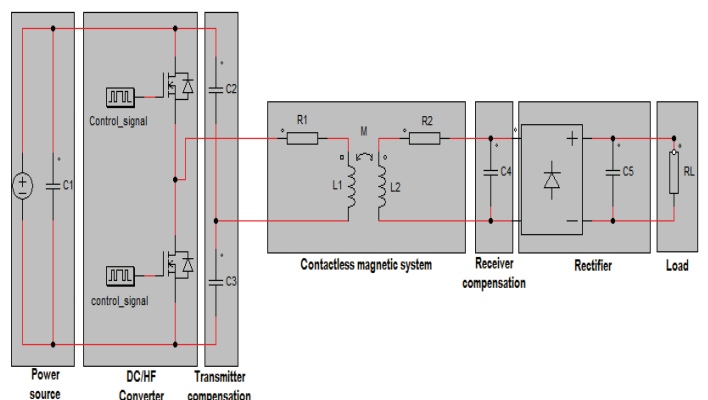


Fig.2. Spatial configuration of the transformer

II. THE ECAM-EPMI'S « ELECTRIC ROAD » PROJECT

The electric vehicle is an excellent solution for reducing greenhouse gas emissions and gaining more independence from oil consumption. However, this interest is altered by the low autonomy of the vehicle's power supply system. Indeed, chemical traction batteries have evolved very slowly in the past 100 years, they are too voluminous (weight, volume) and hardly recyclable. The autonomy reached today for an electric vehicle is hardly of the order of 100 km. In this paper we propose a new technology to remove these limitations. The principle is to install static and/or dynamic fast charging systems on highways and urban infrastructures (Figure 3 (a)).

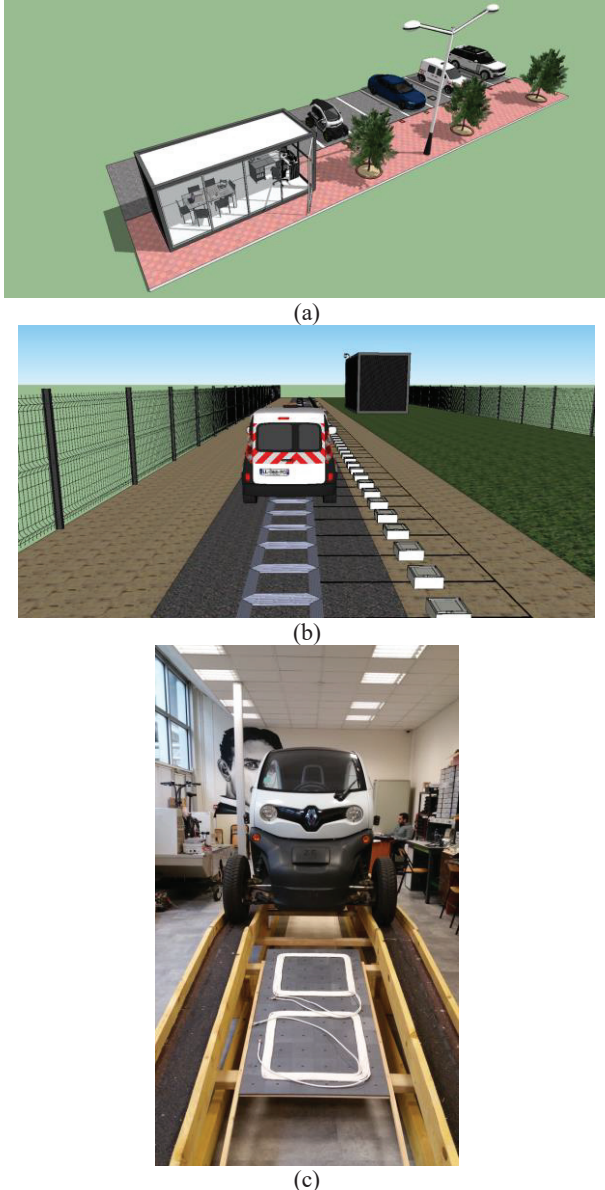


Fig.3. (a) Inductive charging terminals for electric Vehicles, (b) the ECAM-EPMI Electric Road demonstrator, (c) Experimental plant of contactless energy transfer in the Tesla platform

Nevertheless, this causes problems of congestion of the charging places, and even requires reviewing the electricity distribution networks. At the ECAM-EPMI, we propose a dynamic load system, as shown in figure 3(b) and (c), which will be referred to as the "Electric Road". It is a question of placing a system on the ground which, by induction through coils, will supply the moving vehicles. This brings new perspectives that will facilitate the implementation of a driving automation and old ideas such as the grouping of cars in convoy in order to reduce losses due to the displacement of air for a car , And therefore its energy consumption.

III. MUTUEL INDUCTION M

The mutual inductance between two perpendicular wires is zero. This is indeed reflected in the Neumann expression for the mutual inductance between two sections of coils C1 and C2 with respective lengths l1 and l2.

$$M_{12} = \frac{\mu_0}{4\pi l_1 l_2} \oint \frac{dl_1 \cdot dl_2}{r} \quad (1)$$

Where r is the distance between two sections of the coils and μ_0 the permeability of the vacuum.

In this case the inductance is reduced to that of two parallel wires.

$$M_{AB} = \sum_{j=1}^{N_A} \sum_{j=1; j \neq i}^{N_B} m_{a_i b_j} \quad (2)$$

Where $m_{a_i b_j}$ is the mutual inductance between the straight wire a_i of winding A and the straight wire b_j of the winding B.

N_A and N_B are their respective numbers of straight wires.

The mutual inductance between two parallel straight wires, as shown in figure 4, deduced from expression (1) is:

$$M_f = 0.001 [f(l_3 - l_1) - f(l_3 + l_2) + f(l_2 + l_3 + l_1) - f(l_3)]$$

$$\text{Where } f(x) = (x + \sqrt{x^2 + \rho^2}) - \sqrt{x^2 + \rho^2} \quad (3)$$

x and ρ are in cm, M_f in μH [2].

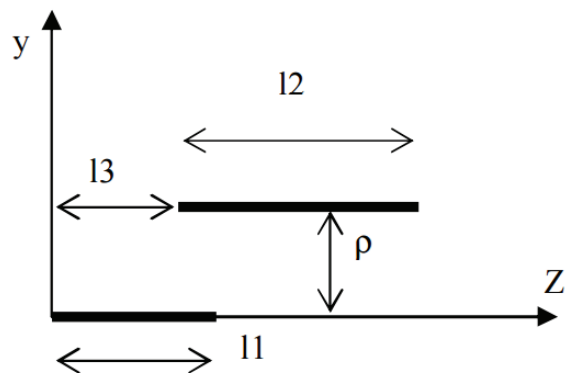


Fig.4. Mutual induction between two parallel wire conductors Mutual induction M

IV. COUPLING COEFFICIENT K

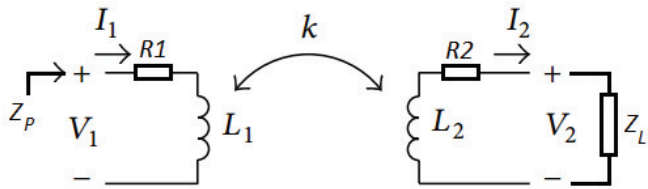


Fig.5. circuit schematic for the inductive link

For a generic load Z_L connected to the secondary coil, the impedance Z_p can be defined as:

$$Z_p = R_1 + j\omega L_1 + \frac{\omega^2 M^2}{j\omega L_2 + R_2 + Z_L} \quad (4)$$

Where R_1 represents the series resistance of L_1 and M the mutual inductance, related to the coupling coefficient K according to:

$$K = \frac{M}{\sqrt{L_1 L_2}} \quad (5)$$

Where L_1 and L_2 are the self-inductance of coils 1 and 2.

The output impedance depends on the inductive coupling coefficient and equations (4) and (5) show this. When M varies, the term $\frac{\omega^2 M^2}{j\omega L_2 + R_2 + Z_L}$, which may have a real and imaginary part, also varies and modifies the impedance Z_p shown in the figure 5.

A. Measurement technique

The equations of the schematic circuit of inductive link shown in figure 5 can be written as

$$V_1 = j\omega(L_1 I_1 + M I_2) \quad (6)$$

$$-V_2 = j\omega(M I_1 + L_2 I_2) \quad (7)$$

If we consider that the secondary coil is shorted, (7) becomes:

$$I_2 = -\frac{M I_1}{L_2} \quad (8)$$

Replacing (8) in (6)

$$V_1 = j\omega I_1(L_1 - \frac{M^2}{L_2}) \quad (9)$$

Assuming:

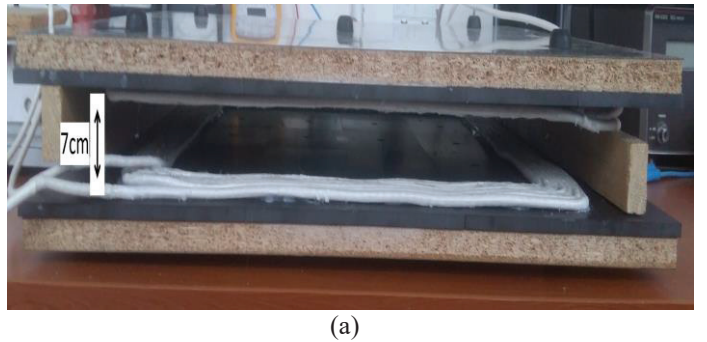
$$L_{SC} = L_1 - \frac{M^2}{L_2} \quad (10)$$

If we set (10) and replacing it with (5), we will have the expression of the coupling coefficient K as a function of the inductance L_1 and the inductance L_{SC} measured when the secondary coil is shorted.

$$K = \sqrt{1 - \frac{L_{SC}}{L_1}} \quad (11)$$

V. EXPERIMENT AND RESULTS

A half bridge resonant converter supplies the primary of the transformer. The primary and secondary are square coils of dimensions 50*50 Cm².



(a)

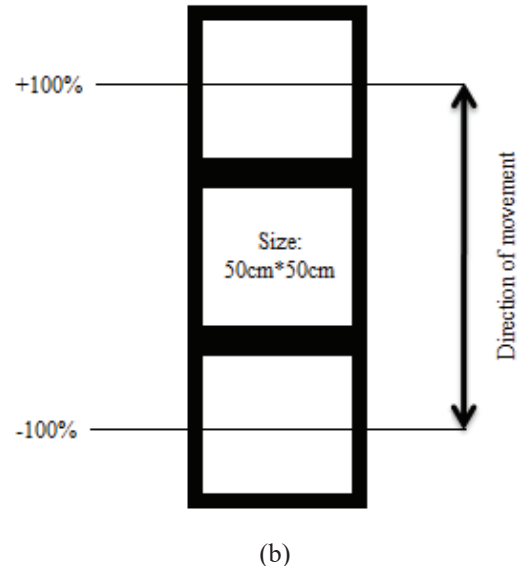


Fig.6. (a) Experimental plant of contactless energy transfer in the Tesla platform, (b) Displacement of the secondary along the Y axis with X = 0

The two coils are made up of 7 turns of cable with an outer diameter of 5 mm. the cable is made by 1500 strands of Litz wire twisted. Both coils are placed on a ferrite field to increase the mutual coupling between them (see figure 6 (a)).

The switching frequency and the supply voltage of the half bridge converter are respectively 54 kHz and 30 V. the switching frequency is the same for both sides and the air gap is 7cm.

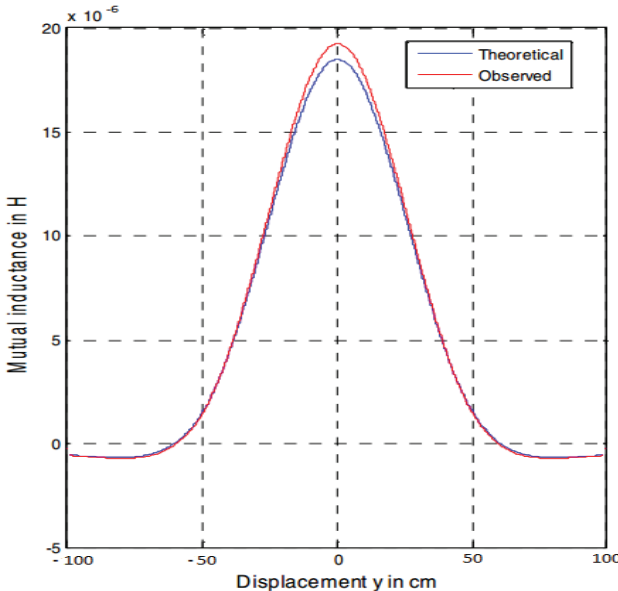


Fig.7. Variation of the mutual inductance as a function of the lateral displacement of the secondary winding $X = 0$, $Z = 7\text{cm}$

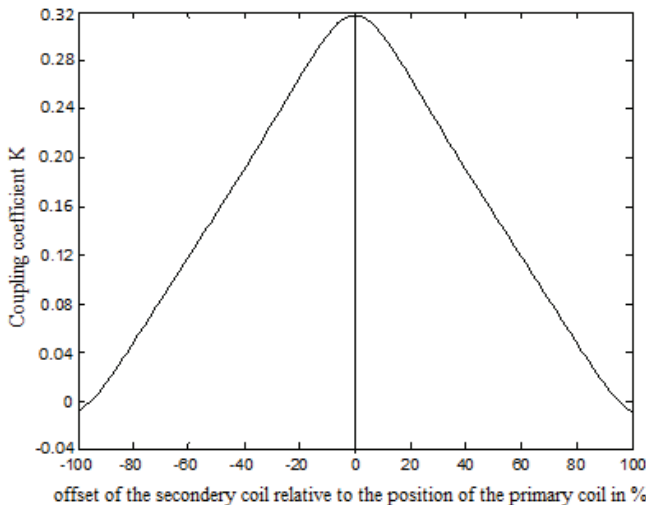


Fig.8. Variation of the coupling coefficient as a function of the lateral displacement of the secondary winding $X = 0$, $Z = 7\text{cm}$

A. Mutual inductance

Theoretical and observed curves of figure 7 show mutual inductance between the winding for displacement along the Y axis with $X=0$ and $Z=7\text{cm}$. The maximum mutual inductance received in the secondary winding is $18\mu\text{H}$, it is obtained when the axis coincide. By doing a shift along the Y-axis, the mutual inductance decreases. The mutual inductance is cancelled for $|Y|=55$ to 60cm . then changes sign and became negative. This is due to the inversely of the current in the secondary.

B. Coupling Coefficient

As shown in Fig. 6 (b), the measurement of the coupling coefficient is made on a displacement from -100% to $+100\%$ of the size of the secondary coil (which is the same size as the

primary coil). The coupling coefficient is maximal and equal to 0.32 when the secondary is centered with respect to the primary. It begins to decrease exponentially during a partial offset and canceled when the secondary and primary are totally off center.

Figures 7 and 8 clearly reflect that the coupling coefficient depends on the mutual inductance; both are in maximum when the primary and secondary axes coincide, decrease almost in the same way during a partial shift and cancel each other when the offset is total.

To optimize the magnetic coupling it is necessary to:

- Increase as much as possible the mutual inductance by optimizing the dimensions of the primary and secondary loops.
- Reduce as much as possible the proper inductances by optimizing the location and shape of the conductors.
- Optimize the distribution of magnetic materials to better channel the magnetic flux.

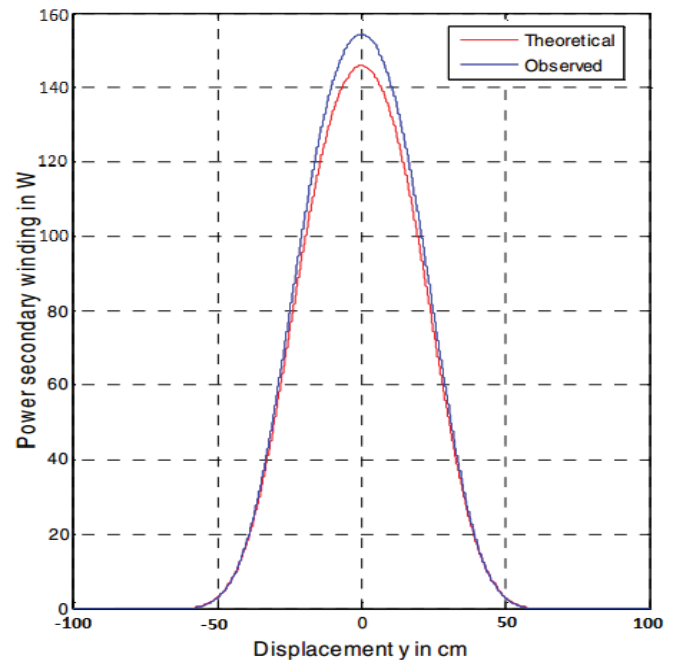


Fig.9. Power in secondary winding versus displacement Y ($X = 0$) for $Z = 7\text{cm}$

C. Secondary power

The maximum power received by the secondary is 150W for a gap of 7 cm and when the axes of the primary and secondary coils coincide (see figure 9). The power of the secondary decreases as the decentration increases, to cancel out when the two coils are totally off center.

We also notice that this power evolution in the secondary is proportional to the evolution of the magnetic inductance and the coupling between the two coils.

VI. CONCLUSION

We present in this article, a wireless energy transmission system through a large air gap, the energy transmission is studied for a chosen distance between the primary and the secondary windings.

This paper illustrated the variation of some parameters in interaction with the magnetic link and how the decentration of secondary coil related to a fixed primary coil can influence the yield of the transformer.

The approach used is based on analytic formulations. The results have been shown to be in good agreement with measurements, thus validating the proposed method.

REFERENCES

- [1] H.Sadki, "Optimisation of electrical energy distribution in future electrical cars," Ph.D. dissertation (in French), Dept. Electric. Eng., Univ. Picardie Jules Verne, 2003.
- [2] N.Hemche, "Study and design of contactless energy and information transfer in embarked Systems," Ph.D. dissertation (in French), Dept. Electric. Eng., Univ. Picardie Jules Verne, 2007.
- [3] Antoine CAILLIEREZ, «Conception d'un système de transfert d'énergie par induction et application au véhicule électrique» (in French), Dept. Electric. EngCentaleSupelec19 janvier 2016.
- [4] A.Caillierez, D. Sadarnac, A. Jaafari, and S. Loudot, "Dynamic inductive charging for electric vehicle: Modelling and experimental results," in 7th IET International Conference on Power Electronics, Machines and Drives (PEMD 2014), 2014, pp. 1–7.
- [5] A.Caillierez, D. Sadarnac, A. Jaafari, and S. Loudot, "Unlimited range for electric vehicles," in 2014 International Symposium on Power Electronics, Electrical Drives, Automation and Motion (SPEEDAM), 2014, pp. 941–946.
- [6] A. Caillierez, P-A. Gori, D. Sadarnac, A. Jaafari, and S. Loudot, "2.4kW prototype of on-road wireless power transfer: modelling concepts and practical implementation" in 18th European Conference on Power Electronics and Applications (EPE 2015), 2015